OPEN

Detection of Reg3γ by Immunohistochemistry in Cerulein-Induced Model of Acute Pancreatic Injury in Mice and Rats

Katherine Shea, MS and Rodney Rouse, DVM, MBA, PhD

Objective: In a continuation of previous work, Reg3γ protein was further evaluated as a biomarker of pancreatic injury using immunohistochemistry in an additional species.

Methods: Mice and rats were treated with intraperitoneal cerulein injections, creating acute pancreatic injury. Mice received 2, 4, or 6 doses, and rats received 1, 2, or 3 doses of cerulein creating low, medium, and high treatment groups. Control animals were dosed with phosphate-buffered saline at corresponding volumes and intervals. Groups of 6 animals were killed 1, 3, 6, 24, and 48 hours after final treatments. Reg3γ immunohistochemical staining and image analysis were performed on pancreatic tissue obtained 6, 24, or 48 hours after control or cerulein treatment. Staining was quantified using image analysis software to calculate area of positivity as a percentage of total tissue area.

Results: Percent positivity of Reg3γ in both species rose by 6 hours, peaked by 24 hours across all 3 cerulein doses, and dropped significantly by 48 hours. In high-dose rats with accompanying gene expression data, Reg3γ gene expression corresponded temporally with quantitative staining data.

Conclusions: Reg3γ staining quantified through image analysis showed a time- and dose-response in cerulein-treated mice and rats.

Key Words: Reg3γ, immunohistochemistry, image analysis

(*Pancreas* 2019;48: 1015–1025)

The regenerating islet-derived 3 (Reg3) family of proteins, α, β, and γ, are C-type lectin-like secretory proteins that have been studied in lung,[1] gastrointestinal tissue,[2,3] and more recently in its role in reducing bacterial translocation from the gut as a protective function for the liver.[4] Reg3 proteins have been studied particularly in the pancreas in which multiple functions or effects of the proteins have been described, including bacterial aggregation, anti-inflammation, acinar to ductal cell metaplasia, and promotion of carcinogenesis from chronic pancreatitis.[5–8] As a group, the Reg3 family has been shown to be associated with acinar cell responses[9] and offer a protective function during acute pancreatitis.[10] In the normal pancreas, Reg3γ staining is absent or very minimally observed as small focal areas of punctate staining in the acinar cells of the exocrine pancreas.[11] During pancreatic injury, there is an increase in presence, amount, and distribution of Reg3γ among acinar cells.[11] Our laboratory has investigated Reg3γ using immunohistochemistry (IHC) in drug-induced pancreatitis in 2 previous rodent studies. In our first IHC evaluation of Reg3γ, a cerulein-induced model of pancreatic injury in mice revealed progressively increasing levels of Reg3γ positive staining in pancreatic tissue from low to high treatment groups.[12] Subsequently, Reg3γ immunohistochemical staining was applied in the evaluation of pancreatic injury induced by exenatide treatment in mice while on a high-fat diet. Immunohistochemistry demonstrated a significantly higher amount of staining in exenatide-treated high-dose animals compared with saline-dosed control animals in a semiquantitative evaluation.[11]

The current study is a follow-up on the previously reported relationship between pancreatic injury and pancreatic Reg3γ staining in drug-induced pancreatitis in mice and examines whether Reg3γ functions as a tissue marker of pancreatic insult in rats as it appears to in mice. Here, tissues from cerulein-treated mice and rats were stained to evaluate the utility of Reg3γ as a tissue-based marker for pancreatic injury and compare staining across species.[13] Compared with our previous work with Reg3γ in pancreatic injury, this study includes a larger number of samples and time points, an increased dose range, and most importantly, an additional species. Reg3γ gene expression in the same experimental samples was also included to correlate with and support the IHC findings. At the time of writing, this is the first published study of Reg3γ IHC and pancreatic injury in rats. This immunohistochemical study expands upon earlier work with Reg3γ and hypothesizes that temporal and dose responses to pancreatic injury can be measured through digital image analysis quantification of Reg3γ IHC staining.

MATERIALS AND METHODS

Study Design

In the in vivo study described in detail in Goodwin et al,[13] different models of drug-induced pancreatitis were used in the evaluation of miR-217 and miR-216a as novel noninvasive biomarkers for acute pancreatic injury. The 3 models, cerulein, L-arginine, and ductal ligation, all produced injury in the exocrine pancreas. The animal experiments were performed according to protocol WO-2012-123 as approved by the White Oak Federal Research Center Institutional Animal Care and Use Committee in adherence to the *Guide for the Care and Use of Laboratory Animals, Eighth Edition*. The current study focuses on the analysis of tissues from the cerulein-treated animals. Cohorts of male C57BL6 mice and Sprague-Dawley rats were dosed by intraperitoneal injection with cerulein at 50 μg/kg concentration at varying frequencies to yield low-, medium-, and high-dose groups. Mice received 2, 4, or 6 doses, and rats received 1, 2, or 3 doses (1 hour between doses in all multidose groups) of cerulein to create the low-, medium-, or high-dose groups, respectively. Control animals

From the Division of Applied Regulatory Science, Center for Drug Evaluation and Research, US Food and Drug Administration, Silver Spring, MD.

Received for publication September 4, 2018; accepted July 11, 2019.

Address correspondence to: Katherine Shea, MS, Division of Applied Regulatory Science, Center for Drug Evaluation and Research, US Food and Drug Administration, 10903 New Hampshire Ave, Bldg 64, Room 2080, Silver Spring, MD 20993 (e-mail: katherine.shea@fda.hhs.gov).

The authors declare no conflict of interest.

DOI: 10.1097/MPA.0000000000001382

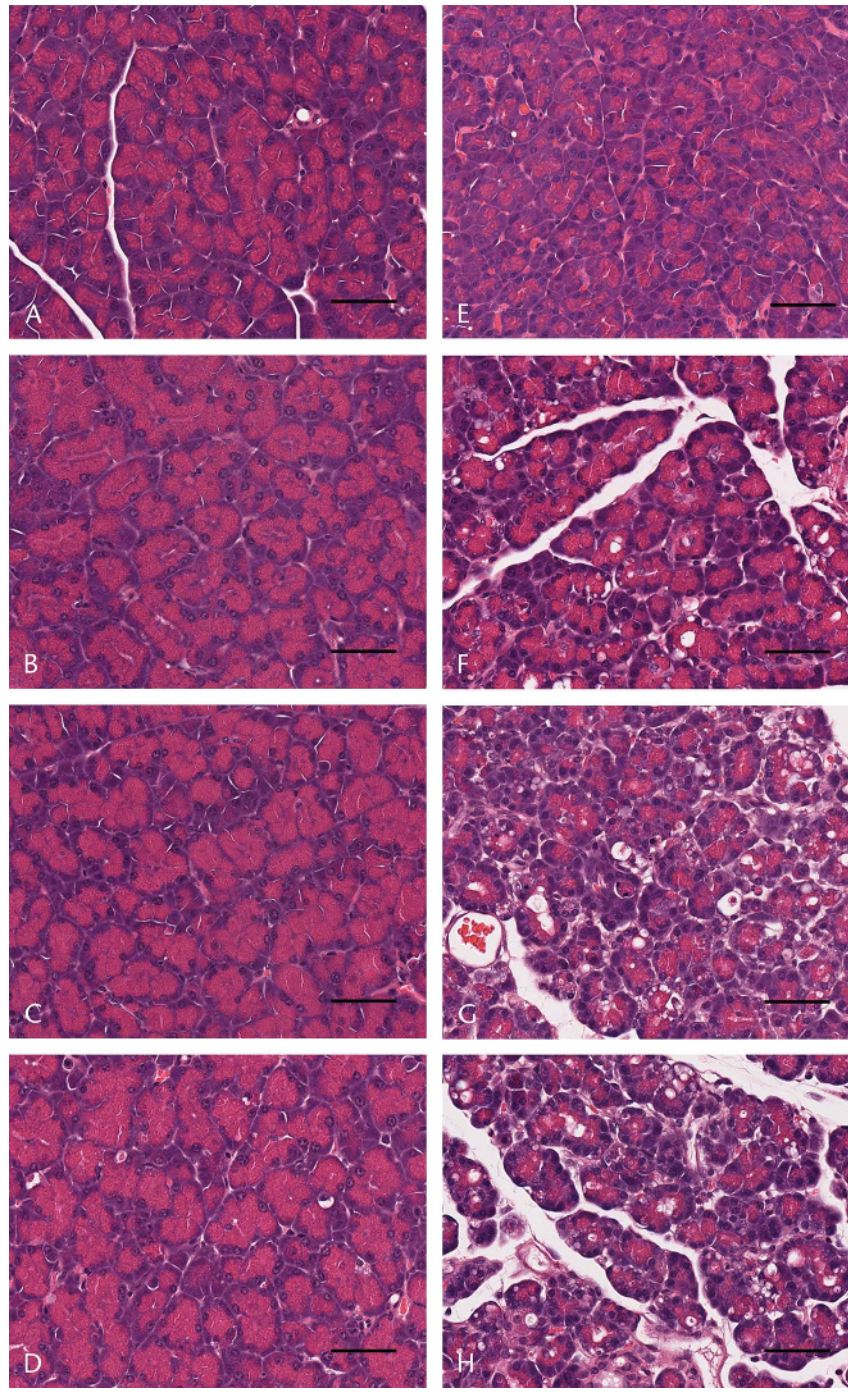

FIGURE 1. Mouse and rat pancreas, H&E by treatment group 24 hours postdose. Mouse: (A) control, (B) low, (C) medium, and (D) high. Rat: (E) control, (F) low, (G) medium, and (H) high. Magnification 40×. Scale bar, 50 μm.

were dosed with Dulbecco's phosphate-buffered saline at corresponding volumes, times, and number of doses. For each dose level, groups of 6 animals were killed via exsanguination under isoflurane-induced anesthesia at 1, 3, 6, 24, and 48 hours after the final cerulein or control treatment. Pancreatic tissues from control and cerulein-treated mice and rats sacrificed at 6, 24, and 48 hours after cerulein administration were divided with a portion for RNA extraction and a portion retained for histopathology as previously reported.[13] Additional tissue sections were made and subjected to IHC staining for Reg3γ followed by digital image analysis.

Histopathology Evaluation

Figure 1 shows hematoxylin and eosin (H&E) images of rat and mouse pancreas from control, low, medium, and high doses obtained 24 hours after treatment. The Reg3γ IHC results were

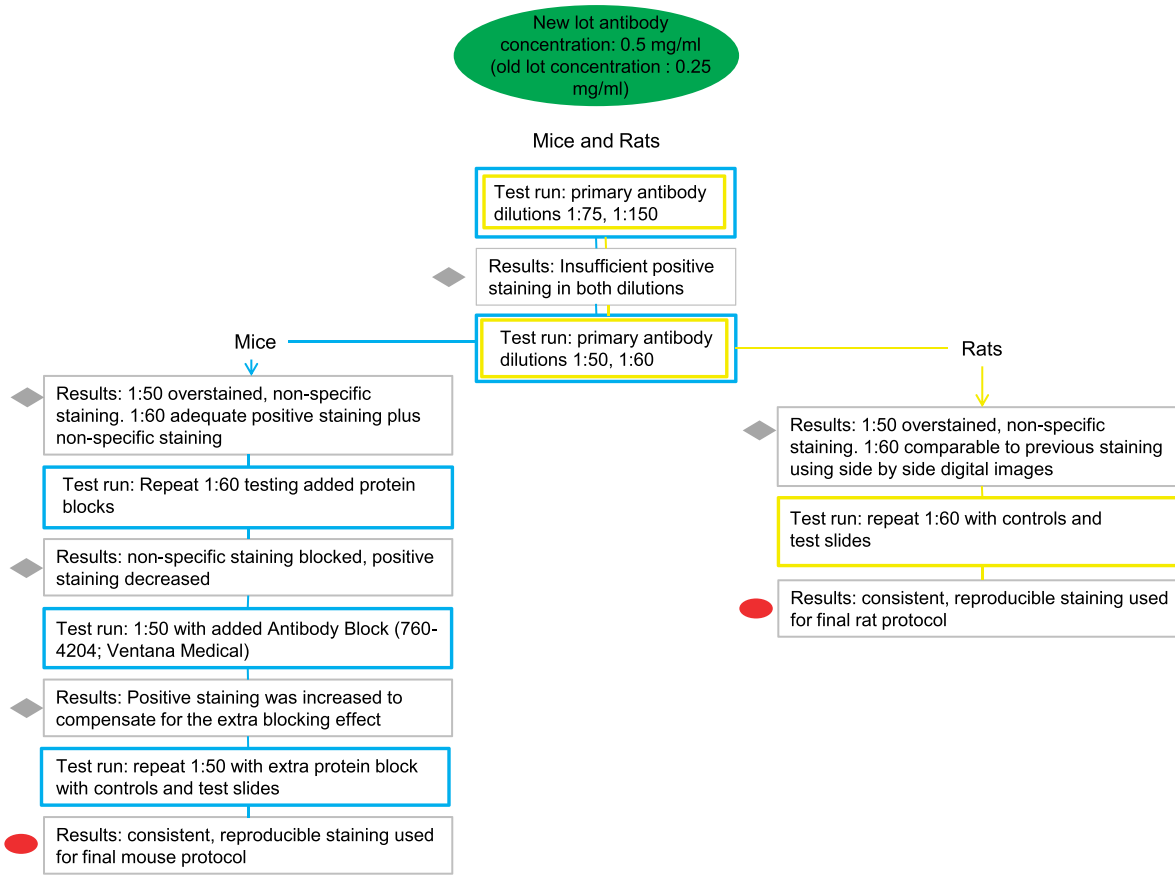

FIGURE 2. New Reg3γ antibody lot workup for mice and rats.

compared with histopathology scoring on H&E slides. Hematoxylin and eosins were scored by a pathologist using criteria outlined in Zhang and Rouse.[14] The pancreas was examined and scored for factors contributing to or characteristics of acinar cell injury of the exocrine pancreas: hypertrophy, autophagy, apoptosis, and necrosis. Scores were also generated for exocrine injury that included damage to parenchyma and adjacent tissues: fat necrosis, vascular injury, interstitial edema, atrophy of acinar lobules, and periductal fibrosis. These evaluations are a subset of histopathology data previously presented graphically.[13]

IHC and Image Analysis

The methods previously described in Rouse et al[11] for Reg3γ IHC staining and image analysis were used in this study. Briefly,

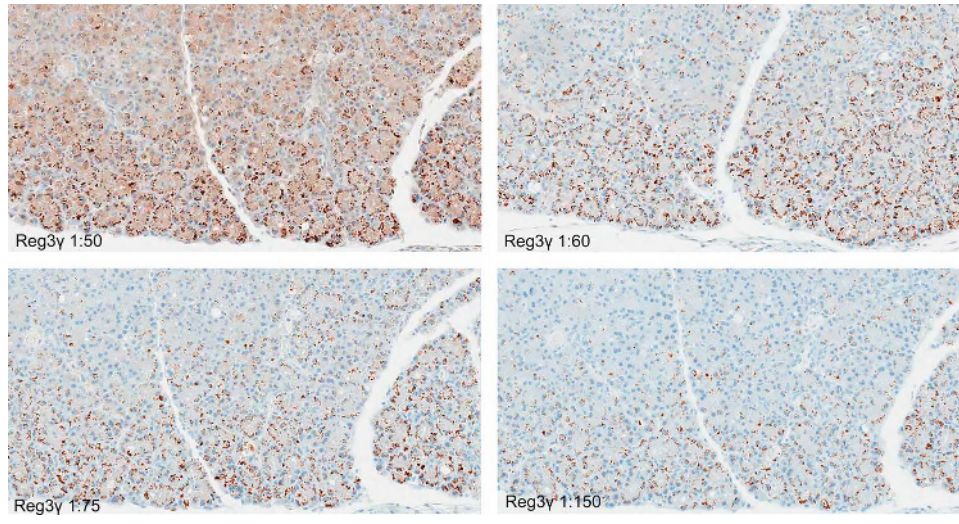

FIGURE 3. Rat positive control pancreas: screen shots of synched images in ImageScope (Aperio) comparing primary antibody dilutions. Images are from nonserial sections of the same block. 1:60 was selected for study slide staining. Magnification 10×.

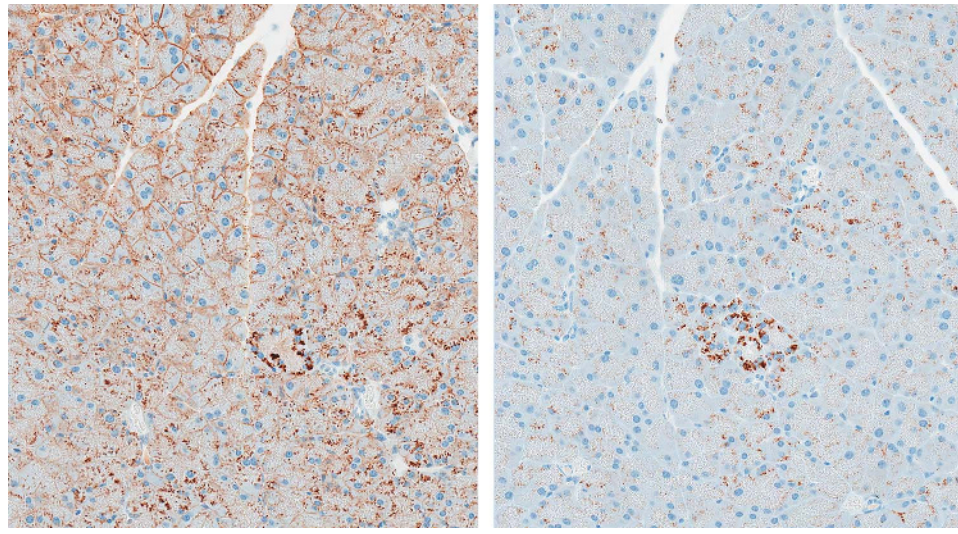

FIGURE 4. Mouse Regγ IHC staining positive control block (nonserial sections of same block). Left, standard staining protocol at 1:60 primary dilution. Right, 1:50 primary antibody dilution with an added protein blocking step to the standard staining protocol to eliminate nonspecific staining. Magnification, 20×.

4 μm sections from formalin-fixed paraffin-embedded tissue blocks were processed from deparaffinization through counterstaining on a DISCOVERY XT (Ventana Medical, Tucson, Ariz) autostainer. Antigen retrieval was performed with 1.5 hours of cell conditioning 1 solution exposure (Ventana Medical). Before antibody application, nonspecific staining was blocked using Antibody Block (Ventana Medical). The rabbit polyclonal Reg3γ antibody (AP5606c; Abgent, San Diego, Calif) was then incubated on the tissue sections for 1 hour at 3 μg/mL, or 10 μg/mL for 48-hour mice and 8.3 μg/mL for 48-hour rats. The primary antibody was then

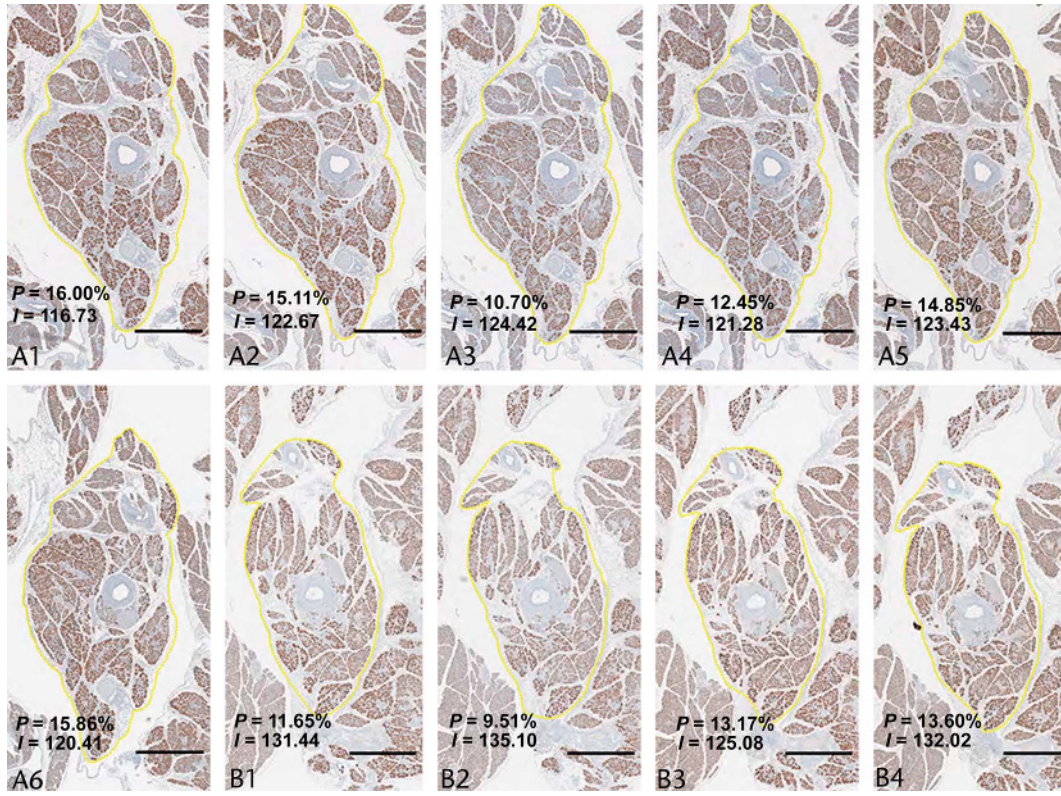

FIGURE 5. Rat control comparison: rat positive control slides from all experimental runs. All control slides are nonserial sections from the same tissue block. A1–A6, control slides for 6- and 24-hour animals (first antibody lot). B1–B4, control slides for 48-hour animals (second antibody lot). Tissue outlined in yellow was used for analysis across lots and runs to yield percent positivity of Reg3γ and average intensity of positive pixels using Aperio Positive Pixel Count Algorithm v9. Percent positivity (*P*) of Reg3γ and average intensity (*I*) are listed on each image. Magnification 1.25×. Scale bar, 1000 μm.

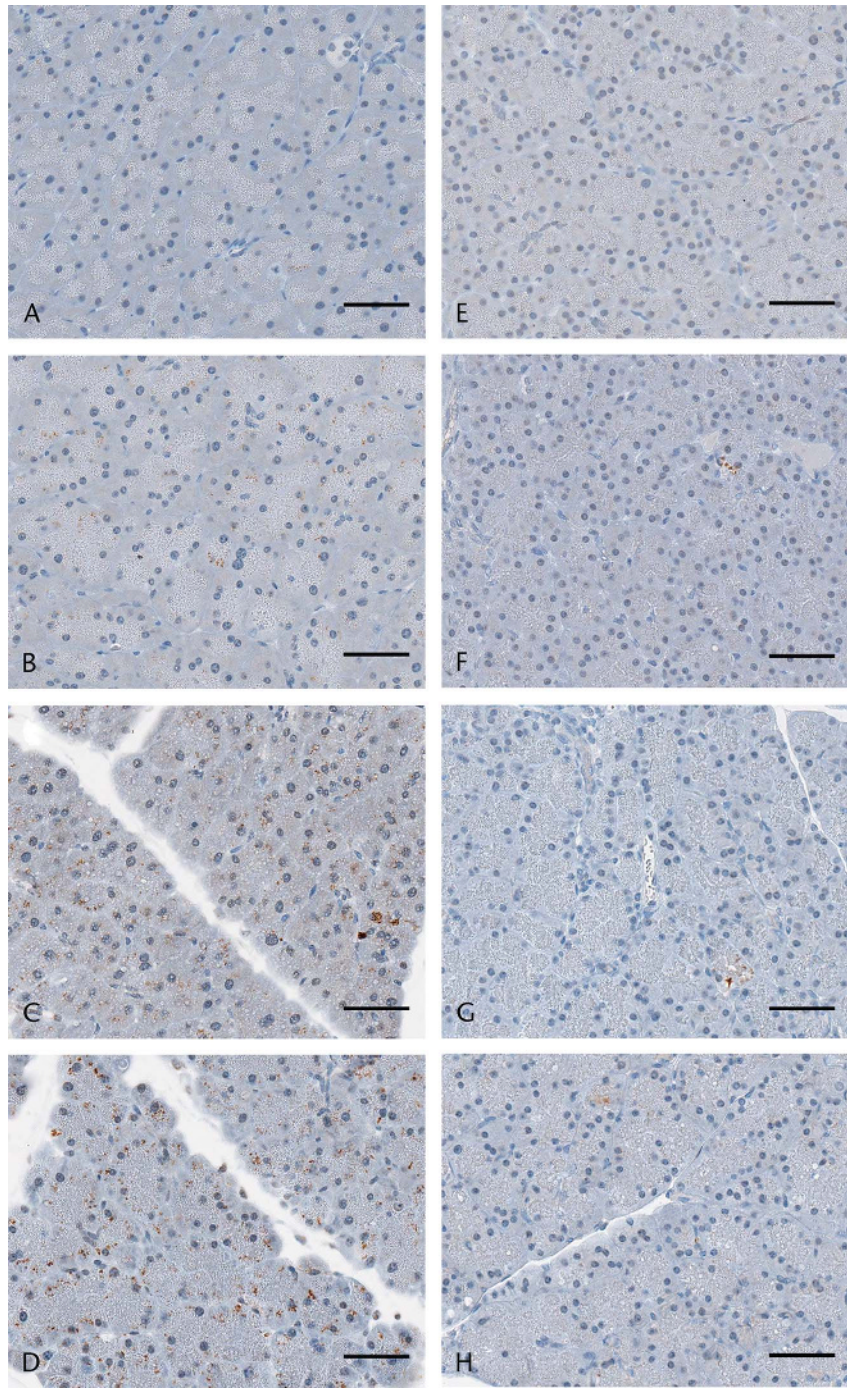

FIGURE 6. Mouse and rat pancreas, Reg3γ IHC by treatment group 6 hours postdose. Mouse: (A) control, (B) low, (C) medium, and (D) high. Rat: (E) control, (F) low, (G) medium, and (H) high. Reg3γ-labeled staining, 3,3'-diaminobenzidine (brown); counterstain, hematoxylin (blue). Magnification 40×. Scale bar, 50 μm.

labeled with a biotinylated goat antirabbit antibody (Vector Laboratories, Burlingame, Calif). Bound antibody was detected and visualized with a DAB Map Detection Kit (Ventana Medical). The primary and secondary antibodies were diluted in Antibody Diluent (Ventana Medical) and 10% Protein Block (Dako, Santa Clara, Calif). Negative controls were run with a rabbit isotype control matched to the concentration of the primary antibody (Sigma-Aldrich, St. Louis, Mo). Based on the results of the 24-hour groups, the 48-hour groups were subsequently stained and processed to see whether Reg3γ expression subsided along with injury at this later time point.

For the inclusion of the 48-hour animals, a new lot of antibody had to be acquired and tested (Figs. 2, 3), resulting in an adjusted working concentration of the primary antibody and an

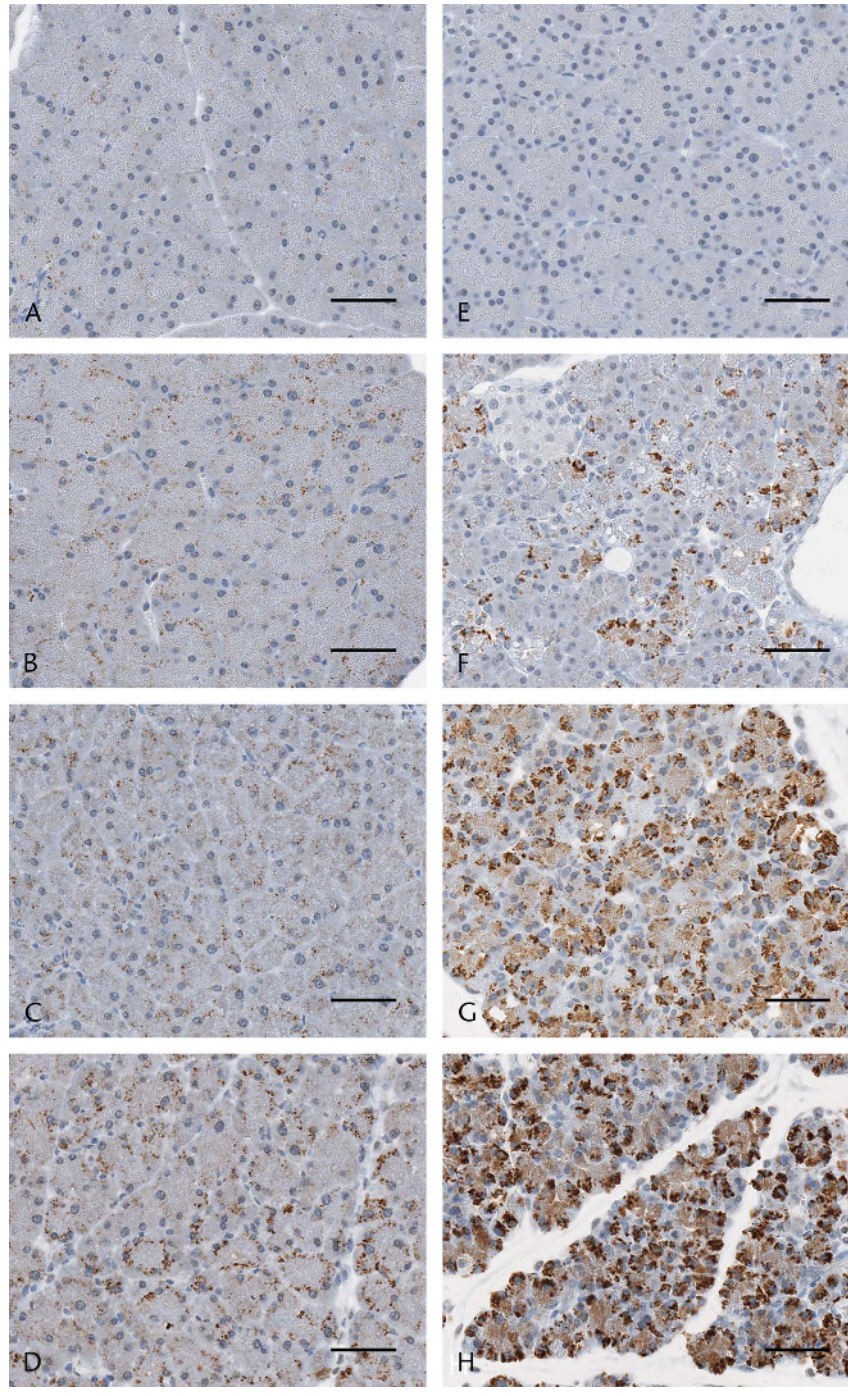

FIGURE 7. Mouse and rat pancreas, Reg3γ IHC by treatment group 24 hours postdose. Mouse: (A) control, (B) low, (C) medium, and (D) high. Rat: (E) control, (F) low, (G) medium, and (H) high. Reg3γ-labeled staining, 3,3'-diaminobenzidine (brown); counterstain, hematoxylin (blue). Magnification 40×. Scale bar, 50 μm.

additional blocking step for mice (Fig. 4) to match previous staining intensity. Test slides were evaluated visually using side by side digital images. The same positive control tissue block (generated from a previous cerulein-induced pancreatitis experiment) was stained using both antibody lots and analyzed for percent positivity of Reg3γ (as described below) and average positive pixel intensity using the Aperio Positive Pixel Count Algorithm v9 (Leica Biosystems, Buffalo Grove, Ill). These measures were used to compare the consistency between the antibody lots and the original and modified staining protocols (Fig. 5).

For quantification, stained slides were scanned on an Aperio CS slide scanner (Leica Biosystems) at 40× with the resulting digital images uploaded into VIS (Visiopharm, Hoersholm, Denmark). The images were processed using a protocol to calculate the area of

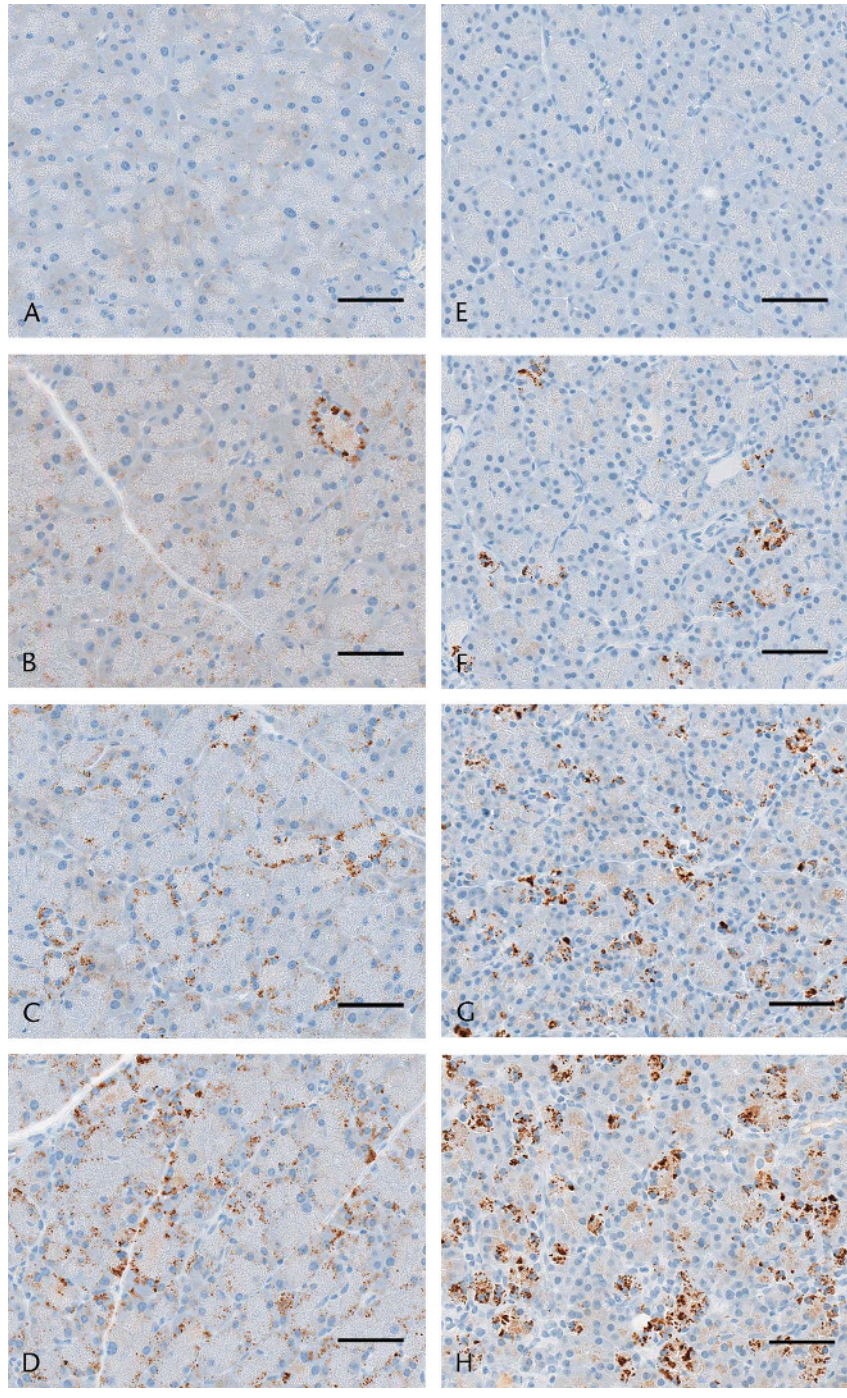

FIGURE 8. Mouse and rat pancreas, Reg3γ IHC by treatment group 48 hours postdose. Mouse: (A) control, (B) low, (C) medium, and (D) high. Rat: (E) control, (F) low, (G) medium, and (H) high. Reg3γ-labeled staining, 3,3'-diaminobenzidine (brown); counterstain, hematoxylin (blue). Magnification 40×. Scale bar, 50 μm.

positivity as a percentage of the total tissue area so that percentages of positivity could be compared across samples. The image analysis protocol used Bayesian classification for image segmentation followed by calculation of the percentage of positive pixel area of the entire segmented image. Before running the image analysis protocol, the entire section of pancreas present on the slide (the region of interest [ROI]) was outlined to establish the total area of tissue. An automated tool was used for ROI detection, which used an edge preserving median filter at 4 times magnification followed by classification of pixel values to determine pancreas and nonpancreas. A threshold of pixel values 223 and below was classified as tissue, and pixel values 224 and above were excluded from the ROI as nonpancreas. Regions of interest were reviewed manually and adjusted to exclude artifacts. Red, green, and blue color channels with

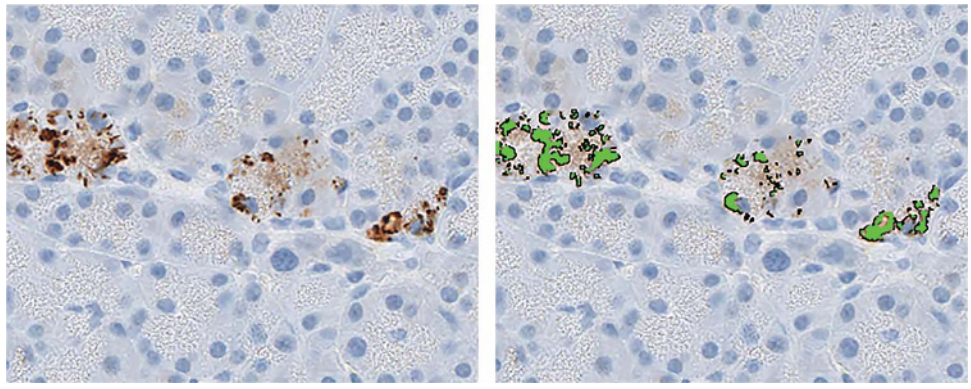

FIGURE 9. Image analysis. Dark brown pixels (left) are classified as positive staining and labeled with a green color (right). Note that lighter staining is not detected as positive and is not labeled with green.

a hematoxylin enhancement were used for image preprocessing. The image was then segmented by pixel color using a pretrained classifier to highlight positive staining 3,3'-Diaminobenzidine (DAB). The classified DAB-labeled area was calculated as a percentage of the total ROI area (μm^2) of analyzed tissue.

Next-Generation Sequencing and Data Processing

Reg3γ IHC results in rats were compared with gene expression data for Reg3γ obtained from the same pancreatic tissue and quantified through next generation sequencing as described in Li and Rouse.[15] Gene expression levels were only determined for the high-dose rats and their control groups. Sequencing of messenger RNA (mRNA) samples and initial quality control bioinformatic analysis were performed by Quintiles, Inc (Morrisville, NC). Briefly, total RNA samples were converted into indexed complementary DNA libraries using TruSeq Stranded Total RNA sample preparation kit and TruSeq Small RNA sample preparation kit (Illumina, San Diego, Calif), respectively. The libraries were quantitated by quantitative polymerase chain reaction, normalized to 2 nM each and sequenced on an Illumina HiSeq platform. For mRNA libraries 2 × 50 bp, paired-end sequencing configurations were used. Eight samples were indexed and pooled together to be run on each lane, which were then demultiplexed after sequencing. Raw sequencing data (sra@ncbi.nlm.nih.gov; accession number SRP095173) was returned to our laboratory after going through Quintiles internal QC steps. In our laboratory, the reads from mRNA samples were aligned to the rat genome (ENSEMBL assembly 5.0) and then quantified using RSEM version 1.2.14.[16]

Statistical Analysis

Mean values of Reg3γ positivity and standard error of the mean (SEM) were calculated in SigmaPlot (Systat Inc, San Jose, Calif), and the means of treated groups were tested to see if they were larger than the mean of the corresponding control groups using a 1-tailed *t* test. Statistical significance was $P \leq 0.05$. In addition, Pearson correlation coefficients were generated to describe the relationship between Reg3γ IHC staining, histopathology composite and component scores, the serum microRNA (miRNA) biomarkers that were the focus of the original study, and Reg3γ gene expression changes. Differential expression analysis for mRNA was done using edgeR.[17] The gene counts from RSEM were upper-quartile normalized and fitted by a general linear model with the group (treatment and time points) effects and other confounding factors as covariates. Messenger RNAs that were differentially expressed between treated and time-matched control samples at any 1 of the 5 time points with a false discovery rate value of less than

TABLE 1. Mouse Reg3γ IHC Image Analysis: Percent Positivity

	6 h	24 h	48 h
Treatment (n = 6)	**Mean ± SEM**	**Mean ± SEM**	**Mean ± SEM**
Low (cerulein 50 μg/kg × 2)	0.256 ± 0.063	1.870 ± 0.157*	1.111 ± 0.194*
Control (saline 50 μg/kg × 2)	0.011 ± 0.002	0.213 ± 0.163	0.006 ± 0.003
Medium (cerulein 50 μg/kg × 4)	0.270 ± 0.142	2.677 ± 0.469*	1.119 ± 0.126*
Control (saline 50 μg/kg × 4)	0.100 ± 0.038	0.719 ± 0.510	0.023 ± 0.011
High (cerulein 50 μg/kg × 6)	0.483 ± 0.324	4.057 ± 0.361*	1.851 ± 0.431*
Control (saline 50 μg/kg × 6)	0.366 ± 0.092	0.756 ± 0.509	0.012 ± 0.004

One-tail *t* test ($P < 0.05$).

*Statistically different from control.

TABLE 2. Rat Reg3γ IHC Image Analysis: Percent Positivity

	6 h	24 h	48 h
Treatment (n = 6)	**Mean ± SEM**	**Mean ± SEM**	**Mean ± SEM**
Low (cerulein 50 μg/kg × 1)	0.008 ± 0.002*	4.177 ± 2.100	2.197 ± 0.989*
Control (saline 50 μg/kg × 1)	0.004 ± 0.001	0.003 ± 0.000	0.002 ± 0.002
Medium (cerulein 50 μg/kg × 2)	0.019 ± 0.011	11.934 ± 1.604*	2.393 ± 0.912*
Control (saline 50 μg/kg × 2)	0.004 ± 0.001	0.002 ± 0.000	0.005 ± 0.002
High (cerulein 50 μg/kg × 3)	0.057 ± 0.018*	15.563 ± 2.333*	2.185 ± 0.739*
Control (saline 50 μg/kg × 3)	0.004 ± 0.001	0.032 ± 0.023	0.002 ± 0.001

One-tail *t* test ($P < 0.05$).

*Statistically different from control.

TABLE 3. Mouse and Rat Reg3γ Percent Positive IHC Correlations to Histology Scores

	Composite Histology	Autophagy	Apoptosis	Necrosis	Atrophy
Mouse					
R	0.455	0.451	−0.0998	0.377	0.281
P	1.36*E*-05	1.70*E*-05	0.366	4.10*E*-04	9.65*E*-03
Rat					
R	0.634	0.512	0.616	0.618	0.574
P	1.69*E*-013	1.77*E*-08	1.61*E*-012	1.39*E*-012	1.05*E*-10

or equal to 0.05 based on the negative binomial model were retained as differentially expressed.

RESULTS

Via standard light microscopy, positive staining was observed as fine punctate dots of chromogen deposition in the cytoplasm of acinar cells of the exocrine pancreas (Figs. 6–8). Larger aggregates of punctate dots were observed in areas of increased pancreatic injury. For image analysis, dark brown pixels were classified as positive (Fig. 9).

Mice

The image analysis data from mice are shown in Table 1. At 6 hours postdose, none of the treatment groups demonstrated staining statistically distinguishable from control animals. At 24 hours posttreatment, the mean percent positive peaked in the range of 1% to 4%, and a statistical difference from corresponding control animals was recognized in all 3 cerulein dosage groups. At this time, each cerulein-treated group reached its maximum level of positivity. By 48 hours posttreatment, mean percent positivity for mice in all dosing groups was lower but remained significantly higher than controls.

Rats

Table 2 shows image analysis data for rats. Very little constitutive Reg3γ IHC staining was observed in rats. By 6 hours posttreatment, mean positivity was elevated in low- and high-dose cerulein groups (although still less than 1%). Variability in the medium dose group precluded statistical significance, although a much higher mean value was obtained compared with controls or even the low-dose cerulein group. By 24 hours posttreatment, rats, similar to mice, had the highest mean levels of positivity with values increasing approximately 4%, 12%, and 16% in low-, medium-, and high-dose groups, respectively, whereas very low levels of positive staining continued to be observed in control rats. The mean positivity of cerulein-treated rats 48 hours after treatment remained significantly elevated compared with controls, in the 2% range for all the dosage groups.

Comparison With Histopathology and Serum Biomarkers

Reg3γ positivity scores determined by image analysis were compared with the semiquantitative histopathology scores generated by a pathologist from the evaluation of H&E slides. The histopathology scores used for comparison included the individual pancreatic injury component scores and the composite score of the 9 components of pancreatic injury. Correlations (*R*) and *P* values of Reg3γ to histology are shown in Table 3 (select data shown). Reg3γ IHC staining results were significantly correlated with the composite histopathology scores with a large correlation coefficient in rats compared with mice. The highest correlation coefficients for mice were composite histology, autophagy, and necrosis. In rats, Reg3γ positivity correlated most strongly with composite histopathology, acinar cell autophagy, apoptosis, necrosis, and atrophy of acinar lobules in rats. Reg3γ staining followed the same trend as the semiquantitative histopathology findings of injury with increased positive staining and scoring noted in rats compared with mice. Although not significantly correlated point to point with serum miR-217, miR-216a, and amylase, Reg3γ staining demonstrated similar time- and dose-induced changes to those observed in those serum biomarkers.[13] Amylase data are shown in Tables 4 and 5. In both mice and rats, serum amylase concentrations were elevated at 6 hours postdose and slightly

TABLE 4. Mouse Serum Amylase Concentrations, U/L

	6 h	24 h	48 h
Treatment (n = 6)	**Mean ± SEM**	**Mean ± SEM**	**Mean ± SEM**
Low (cerulein 50 μg/kg × 2)	63,425 ± 4611*	23,910 ± 863	19,955 ± 566
Control (saline 50 μg/kg × 2)	16,528 ± 1140	22,029 ± 1695	20,718 ± 652
Medium (cerulein 50 μg/kg × 4)	81,131 ± 11,467*	20,775 ± 1810	18,789 ± 1278
Control (saline 50 μg/kg × 4)	41,523 ± 12,251	19,605 ± 2070	19,148 ± 1186
High (cerulein 50 μg/kg × 6)	64,235 ± 5762*	32,187 ± 3313*	15,426 ± 541
Control (saline 50 μg/kg × 6)	17,743 ± 608	20,064 ± 1222	18,386 ± 1334

One-tail *t* test ($P < 0.05$).

*Statistically different from control.

TABLE 5. Rat Serum Amylase Concentrations, U/L

	6 h	24 h	48 h
Treatment (n = 6)	**Mean ± SEM**	**Mean ± SEM**	**Mean ± SEM**
Low (cerulein 50 μg/kg × 1)	126,312.22 ± 20,896.18*	29,718.85 ± 4200.53	13,745.83 ± 1007.00
Control (saline 50 μg/kg × 1)	19,480 ± 2522	20,697 ± 1720	14,028 ± 2055
Medium (cerulein 50 μg/kg × 2)	94,208.15 ± 21,710.29*	29,453.51 ± 1992.75	14,969.78 ± 2122.44
Control (saline 50 μg/kg × 2)	22,941 ± 1394	23,616 ± 2904	14,687 ± 1624
High (cerulein 50 μg/kg × 3)	120,610.86 ± 11,812.49*	24,146.57 ± 1967.87	11,109.65 ± 918.62
Control (saline 50 μg/kg × 3)	17,240 ± 1155	22,289 ± 4820	11,524 ± 1020

One-tail *t* test ($P < 0.05$).

*Statistically different from control.

elevated at 24 hours after treatment and were at control levels by 48 hours postdose.[13]

Comparison With Gene Expression in Rats

Gene expression levels of Reg3γ in high-dose rats were compared with percent positivity of Reg3 IHC staining and histology scores (Table 6). Gene expression was significantly correlated with atrophy, composite histology score, apoptosis, Reg3γ IHC percent positivity, and autophagy. The differential gene expression of Reg3γ (Table 7) showed a log fold change of 3.17 at 6 hours postdose, rose to 9.85 at 24 hours postdose before falling to 7.45 by 48 hours after treatment.

DISCUSSION

Previously, a dose response in acute pancreatic injury was demonstrated in mice using Reg3γ IHC.[11,12] The current study agrees with those studies and shows that in both mice and rats percent positivity of Reg3γ increased from low to high injury. Reg3γ detection rose, peaked, and then declined over 48 hours with the highest Reg3γ levels detected at 24 hours. The Reg3γ pattern of expression and percent positivity over time and dose aligns with the measured serum biomarkers of acute pancreatic injury (serum miR-217, miR216a, and amylase). Although Reg3γ results followed the same patterns of injury evolution and resolution, there was no point to point correlation with the serum miRNAs (miR-217, miR216a) under investigation in the original study or serum amylase, the classical indicator of pancreatic injury. Reg3γ staining had higher correlations to histopathology than did the miRNAs. For mice, the higher percentages of staining in control animals compared with rat controls capture the observation in the original study that mouse controls had higher miRNA and histopathology scores, possibly an effect of repeated intraperitoneal saline injections.[13] Reg3γ staining also reflects the earlier finding that rats are more susceptible to pancreatic injury than mice across several models of pancreatic injury.[13]

In the Goodwin et al[13] study, pancreatic injury was induced by cerulein treatment to measure biomarker sensitivity and specificity; therefore, the injury was designed to be mild and focal, not reaching the level of inflammation indicative of acute pancreatitis (see histopathology scoring methodology for the models[14]). When cerulein-treated groups were compared with their respective control groups at 24 hours and 48 hours in this IHC study, most cerulein-treated groups were statistically elevated from their control groups, even at low positivity levels (1%–2% at 48 hours). Digital image analysis of Reg3γ expression was sensitive enough to demonstrate a time- and dose-response even in this environment of subtle injury.

Because of the nature of the cytoplasmic staining pattern, image analysis for this study was designed to capture the area of stained particles. Size and distribution of stained punctate dots varied from fine, sparse, and distinct to amassed aggregates. Because of the irregular shape of the pancreas, an ROI detection protocol using a combination of smoothing and threshold filters outlined the tissue and excluded any adjacent tissue such as lymph node. Areas containing artifacts (such as folds or wrinkles) on stained slides were excluded manually to avoid false positives from image analysis using a clear polygon drawing tool. The resulting area was used as the total pancreas area with positivity expressed as a percentage of that area.

Technical challenges of this study included the availability and concentration of primary antibody. Initially, 6- and 24-hour groups were included in the study, but with definitive positive staining performance, the 48-hour groups were added. The 1- and 3-hour groups were not included because the time elapsed after treatment was not anticipated to be sufficient to allow for changes in protein expression. The relatively small changes detected at 6 hours support the exclusion of the earlier time points. Besides the 48-hour animals, all other time points in both mice and rats were completed with the same lot of primary antibody. Although the antibody discontinuity was not ideal, viable and comparative staining results were obtained. This ability to detect injury across antibody lots further supports the viability of Reg3γ as a tissue biomarker of acinar cell injury.

Gene expression data for the high-dose rats and their controls were obtained from a separate study generated from the same experimental animals and reported by Li and Rouse.[15] Next-generation

TABLE 6. Rat Reg3γ Gene Expression Correlations to Reg3γ % Positivity and Histology Scores

	Reg3γ % Positivity	Composite Histology	Autophagy	Apoptosis	Necrosis	Atrophy
Rat high dose						
Correlation coefficient	0.587	0.718	0.572	0.639	0.443	0.792
P	1.65*E*-04	8.11*E*-07	2.71*E*-04	2.77*E*-05	6.77*E*-03	8.76*E*-09

TABLE 7. Rat Reg3γ Differential Gene Expression Statistics

	6 h	24 h	48 h
Rat high dose			
Log fold change above control	3.17	9.85	7.45
False discovery rate	0.02	4.42*E*-08	6.38*E*-05

False discovery rate, ≤0.05.

sequencing was used to determine gene expression levels in the cerulein-treated rats in comparison with control rats across a time series, and the resulting Reg3γ data was extracted to support the present study. Gene expression in log fold change above control exhibited the same trend and was significantly correlated with IHC percent positive results across all time points. Independently generated gene expression and protein detection levels of Reg3γ support Reg3γ as a tissue biomarker of pancreatic injury with a possible linked to the processes of apoptosis and atrophy.

CONCLUSIONS

Immunohistochemical staining with Reg3γ quantified through image analysis showed a time- and dose-response in cerulein-treated mice and rats. Overall, staining in mice and rats performed similarly but with a stronger response in rats. The percent positive Reg3γ staining in both species peaked at the 24-hour time point across all 3 cerulein doses and dropped significantly by 48 hours. Rat pancreatic injury was detected for the first time with Reg3γ IHC staining. Time and dose characteristics in Reg3γ staining were supported by very similar temporal trends in gene expression of Reg3γ in high-dose rats and in serum biomarkers of acinar cell injury: miR-217, miR216a, and amylase. Reg3γ IHC successfully reflected acute pancreatic injury in formalin-fixed paraffin-embedded tissue sections.

REFERENCES

1. Choi SM, McAleer JP, Zheng M, et al. Innate Stat3-mediated induction of the antimicrobial protein Reg3gamma is required for host defense against MRSA pneumonia. *J Exp Med*. 2013;210:551–561.
2. Vaishnava S, Yamamoto M, Severson KM, et al. The antibacterial lectin RegIIIgamma promotes the spatial segregation of microbiota and host in the intestine. *Science*. 2011;334:255–258.
3. Loonen LM, Stolte EH, Jaklofsky MT, et al. REG3γ-deficient mice have altered mucus distribution and increased mucosal inflammatory responses to the microbiota and enteric pathogens in the ileum. *Mucosal Immunol*. 2014;7:939–947.
4. Wang L, Fouts DE, Stärkel P, et al. Intestinal REG3 lectins protect against alcoholic steatohepatitis by reducing mucosa-associated microbiota and preventing bacterial translocation. *Cell Host Microbe*. 2016;19:227–239.
5. Iovanna J, Orelle B, Keim V, et al. Messenger RNA sequence and expression of rat pancreatitis-associated protein, a lectin-related protein overexpressed during acute experimental pancreatitis. *J Biol Chem*. 1991; 226:24664–24669.
6. Huan C, Kim D, Ou P, et al. Mechanisms of interleukin-22's beneficial effects in acute pancreatitis. *World J Gastrointest Pathophysiol*. 2016;7: 108–116.
7. Li Q, Wang H, Zogopoulos G, et al. Reg proteins promote acinar-to-ductal metaplasia and act as novel diagnostic and prognostic markers in pancreatic ductal adenocarcinoma. *Oncotarget*. 2016;7:77838–77853.
8. Yin G, Du J, Cao H, et al. Reg3g promotes pancreatic carcinogenesis in a murine model of chronic pancreatitis. *Dig Dis Sci*. 2015;60:3656–3668.
9. Keim V, Iovanna JL, Rohr G, et al. Characterization of a rat pancreatic secretory protein associated with pancreatitis. *Gastroenterology*. 1991;100: 775–782.
10. Zhang H, Kandil E, Lin YY, et al. Targeted inhibition of gene expression of pancreatitis-associated proteins exacerbates the severity of acute pancreatitis in rats. *Scand J Gastroenterol*. 2004;39:870–881.
11. Rouse R, Zhang L, Shea K, et al. Extended exenatide administration enhances lipid metabolism and exacerbates pancreatic injury in mice on a high fat, high carbohydrate diet. *PloS One*. 2014;9:e109477.
12. Zhang L, Zhang J, Shea K, et al. Autophagy in pancreatic acinar cells in caerulein-treated mice: immunolocalization of related proteins and their potential as markers of pancreatitis. *Toxicol Pathol*. 2014;42: 435–457.
13. Goodwin D, Rosenzweig B, Zhang J, et al. Evaluation of miR-216a and miR-217 as potential biomarkers of acute pancreatic injury in rats and mice. *Biomarkers*. 2014;19:517–529.
14. Zhang J, Rouse RL. Histopathology and pathogenesis of caerulein-, duct ligation-, and arginine-induced acute pancreatitis in Sprague-Dawley rats and C57BL6 mice. *Histol Histopathol*. 2014;29:1135–1152.
15. Li Z, Rouse R. Co-sequencing and novel delayed anti-correlation identify function for pancreatic enriched microRNA biomarkers in a rat model of acute pancreatic injury. *BMC Genomics*. 2018;19:297.
16. Li B, Dewey C. RSEM: accurate transcript quantification from RNA-Seq data with or without a reference genome. *BMC Genomics*. 2011;12:323.
17. Robinson MD, McCarthy DJ, Smyth GK. edgeR: a Bioconductor package for differential expression analysis of digital gene expression data. *Bioinformatics*. 2010;26:139–140.